Accepted Manuscript

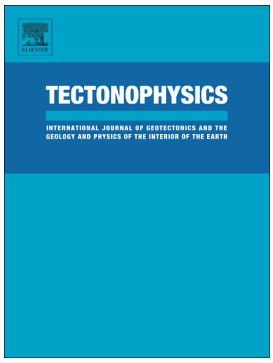

Structural interpretation of El Hierro (Canary Islands) rifts system from gravity inversion modelling

S. Sainz-Maza, F.G. Montesinos, J. Martí, J. Arnoso, M. Calvo, A. Borreguero

PII: S0040-1951(17)30194-4
DOI: doi: 10.1016/j.tecto.2017.05.010
Reference: TECTO 127486

To appear in: *Tectonophysics*

Received date: 4 January 2017
Revised date: 3 May 2017
Accepted date: 14 May 2017

Please cite this article as: S. Sainz-Maza, F.G. Montesinos, J. Martí, J. Arnoso, M. Calvo, A. Borreguero , Structural interpretation of El Hierro (Canary Islands) rifts system from gravity inversion modelling, *Tectonophysics* (2017), doi: 10.1016/j.tecto.2017.05.010

Structural Interpretation of El Hierro (Canary Islands) rifts system from gravity inversion modelling

S. Sainz-Maza[1*)], F. G. Montesinos[2,5)], J.Martí[3)] J. Arnoso[4)5)], M. Calvo[1)], A. Borreguero[1)]

[1)] Observatorio Geofísico Central (IGN). C/ Alfonso XII, 3. 28014 Madrid, Spain.

[2)] Facultad de Matemáticas. Universidad Complutense de Madrid. Plaza de Ciencias, 3. 28040 Madrid, Spain.

[3)] Instituto de Ciencias de la Tierra *Jaume Almera* (CSIC). C/ Lluís Solé i Sabarís s/n, 08028 Barcelona, Spain.

[4)] Instituto de Geociencias (CSIC, UCM). Ciudad Universitaria. Plaza de Ciencias, 3. 28040 Madrid, Spain.

[5)] Grupo Geodesia-UCM, Madrid, Spain.

*) Corresponding author

Sergio Sainz-Maza Aparicio

e-mail: ssainz-maza@fomento.es. Tel. +34 917929437

Submitted for publication:

Tectonophysics

Keywords: El Hierro; Rift system; Gravity inversion.

Abstract

Recent volcanism in El Hierro Island is mostly concentrated along three elongated and narrow zones which converge at the centre of the island. These zones with extensive volcanism have been identified as rift zones. The presence of similar structures is common in many volcanic oceanic islands, so understanding their origin, dynamics and structure is important to conduct hazard assessment in such environments. There is still not consensus on the origin of the El Hierro rift zones, having been associated with mantle uplift or interpreted as resulting from gravitational spreading and flank instability. To further understand the internal structure and origin of the El Hierro rift systems, starting from the previous gravity studies, we developed a new 3D gravity inversion model for its shallower layers, gathering a detailed picture of this part of the island, which has permitted a new interpretation about these rifts. Previous models already identified a main central magma accumulation zone and several shallower high density bodies. The new model allows a better resolution of the pathways that connect both levels and the surface. Our results do not point to any correspondence between the upper parts of these pathways and the rift identified at the surface. Non clear evidence of progression towards deeper parts into the volcanic system is shown, so we interpret them as very shallow structures, probably originated by local extensional stresses derived from gravitational loading and flank instability, which are used to facilitate the lateral transport of magma when it arrives close to the surface.

1. Introduction

Basaltic volcanism in volcanic islands is in most cases controlled by rift systems that represent preferential intrusion paths at the shallowest levels of such volcanic environment (Walker, 1999). These rift structures determine the location of volcanic vents appearing at surface as alignments of cones and eruptive fissures. Rift systems have been identified in many oceanic volcanic islands and large volcanoes, such as Hawaii (Fiske and Jackson, 1972), Canary Islands (Carracedo, 1994), Reunion (Carter et al., 2007; Bonali et al., 2011), Galapagos (Lonsdale, 1988), Etna (Rittmann, 1973; Corazzato and Tibaldi, 2006) or Stromboli (Tibaldi et al., 2003). Discussion about the origin and persistency of the rift zones in basaltic volcanoes still continues, and several models have been proposed, such as a direct relation with pre-existing lithospheric faults, hotspot-related crustal doming, volcanic load and spreading and flank instabilities (MacDonald, 1972; Carracedo, 1994; Walker, 1999; Walter and Troll, 2003; Walter et al., 2005; Lipman and Calvert, 2011; Tibaldi et al 2014, Michon et al., 2015). Simultaneously, the internal structure of the rift systems is also unclear: there is no general agreement on whether they act as shallow structures, managing the magma transport from few km deep below the surface, or by contrast the rift systems drive the magma from the deepest parts of the volcanic system (Walker, 1999; Amelung et al., 2007; Tibaldi et al., 2014; Michon et al., 2015).

Rift systems have been identified in some of the islands of the Canary archipelago as Lanzarote, Tenerife, La Palma and El Hierro (Carracedo, 1994). There is a general agreement that they have controlled the location of Quaternary volcanism. However, it is still unclear what is their origin and what is their internal structure in relation to the whole volcanic edifice. In this sense, rift structures in the Canary Islands have been interpreted as resulting from mantle uplift (Carracedo, 1994), or as resulting from gravity-driven lateral escape of island segments, induced by loading of the deformable substratum (Walter, 2003), or as structures that were

already present in the oceanic basement and have controlled fissural volcanism along the whole history or the archipelago (Anguita and Hernan, 2000). Depending on the interpretation given, these rift structures may be considered either as shallow (e.g.: Becerril et al 2015) or as deeply rooted structures (e.g.: Carracedo, 1994), having then different implications on magma transport inside the Canarian volcanic edifices.

Recent studies using paleomagnetic data in the island of Tenerife (Soriano et al., 2008, Delcamp et al., 2010, 2014) have allowed understanding the relative time relationship between distinct dykes groups, as well as certain structural constraints on the rift-zone development and magma flow patterns. Furthermore, detailed field studies on dike orientations along rift zones have contributed to understand the potential relationships between rift evolution and large sector collapses, and how the previous stages to these gravitational collapses, as the creeping before a collapse, drives the subsequent orientation for the dykes emplacement (Carracedo et al., 2011; Delcamp et al., 2012 and 2014). However, the internal structure of the rift zones is still unknown and it is not clear. It is not yet well understood if they act as channels for magma to ascent from deep reservoirs to shallow zones, indicating that they would be deep rooted structures or by contrast, if they act as shallow structures, only representing pathways for the lateral migration of magma once it has been emplaced at shallow levels in the volcanic system.

Here, we present a new study focused on the rift systems of El Hierro Island based on gravity data. This study complements previous researches done by inversion of gravity data on El Hierro Island (Montesinos et al., 2005a and 2006; Gorbatikov et al. 2013). The onshore gravity values provided by Montesinos et al. (2005a; 2006) were supplemented with 248 new field observations (Figure 1), collected in successive campaigns between 2012 and 2014. All data were used to build the corresponding Bouguer anomaly map, which was calculated using a more precise digital terrain model and a more detailed bathymetry of the surrounding areas than in previous works. This allowed us to obtain more precise terrain corrections to our data.

Bouguer anomalies data were transformed into a 3D model of distribution of density contrasts using a genetic algorithm for gravity inversion (Montesinos et al., 2005b). We obtained a new accurate model of the shallowest part of El Hierro volcanic system, which reaches a depth of 7 km b.s.l. This model is the main argument for our further discussion where we compare it with the information and results obtained from previous studies aiming to a better knowledge of the rift system in El Hierro.

2. Background information.

El Hierro is located in the western-most part of the Canarian Archipelago (Figure 1). This island is the smallest one of the Canary Islands (269 km^2), and started to emerge about 1.2 Ma ago above sea level, rising from a 3.7-4.0 km deep ocean floor. Three volcanic edifices, Tiñor, El Golfo and Las Playas, have been shaped the island surface and were built through episode of intense activity followed by instability periods with lateral collapses such as those of Las Playas, El Julan and El Golfo (Masson, 1996; Urgeles et al., 1997; Gee et al., 2001) (Figure 1). These growth/collapse episodes, combined with a slow erosive rate resulted in a sharp topography which reaches a maximum elevation of 1501 m a.s.l. at Malpaso peak (Figure 1). Due to its short geologic age, and to the aforementioned slow erosive rate acting on it, a high number of well-preserved monogenetic volcanic edifices can be observed at the surface of the island. Despite being currently in a growing phase, according to the radiometric dating and magnetic stratigraphy (Guillou et al., 1996), its activity rate during the Holocene seems to be reduced to a few onshore eruptions, such as the Tanganasoga one, dated at about 6.7 ky (Pellicer, 1977) and Montaña Chamuscada eruption, dated at about 2.5 ky (Guillou et al., 1996). Seismic crisis of 1793, which was related to Lomo Negro eruption, placed at the westernmost part of the island (Hernández-Pacheco, 1982), has been recently discarded as the precursor of that onshore eruption by Villasante-Marcos and Pavón-Carrasco (2014). Instead, the last

submarine eruption occurred in 2011-2012 (López et al., 2012, Martí et al., 2013), characterized by a high seismic activity without an onshore volcanic culmination, as well as the large amount of submarine volcanic cones around the island (Becerril et al., 2016), suggest that recent offshore eruptions could be more frequent than previously thought.

The main features of the internal structure of El Hierro have been inferred using different geophysical techniques and their corresponding data inversion methodologies. Gravimetry (Montesinos et al., 2005a; 2006), microseismic soundings (Gorbatikov et al., 2013) and seismic tomography (García-Yegüas et al., 2014) proposed the existence of a deep-rooted central core, which compounds the main central structure of the island. It is characterized by a high positive density contrast and a positive anomaly for the seismic wave's velocities (Montesinos et al., 2005a; 2006; Gorbatikov et al., 2013). In turn, shallower levels are also composed of several high-density contrast bodies at depths of between 500 and 3000 m b.s.l.

There is certain controversy concerning nature and number of rifts present in each island. (Carracedo, 1996; Carracedo et al., 2001; Münn et al. 2006; Blanco-Montenegro et al., 2008). While some authors consider that during the growing of the volcanic edifices is usual that the uplift force of the ascending magma breaks the crust following a minimal stress configuration of 120^{o} between the respective generated fractures and that these are used by the magma to ascend to surface, others consider that there is not evidence supporting such a "three armed" configuration and that these structures are vertically deep-rooted in the crust (Montesinos et al., 2005a; 2006; Geyer and Martí, 2010; Gorbatikov et al., 2013; García-Yegüas et al. 2014; Becerril et al., 2015). In fact, the density contrast model obtained by Montesinos et al. 2005a and 2006, reveals shallower low-density alignments parallel with the rift directions, these structures being interpreted as resulting from recent extensional fracturing and volcanism. Moreover, Gorbatikov et al., 2013, suggested that El Hierro rifts are the result of the merging of volcanic edifices at surface, in a similar way to the model proposed by Münn

et al., 2006. They explain that the rift configuration is controlled by gravitational spreading of the consecutively overlapping volcanic edifices. Recently, Becerril et al., 2015, characterized the shallower structure of El Hierro Island through the study of the interior of seventeen water galleries. They found that structural elements such as dykes and eruptive fissures followed radial pattern. This pattern may result from a combination of loading, gravitational spreading and magma-induced upwelling, with some influence of previous regional structures. According to them, radial configuration was masked by the giant landslides occurred in the past, which shaping the island with the current three-armed rift system appearance, interpreting the rift zones of El Hierro as shallow structures. The shallower character of the rift structures seems increasingly evident, having been postulated distinct surface mechanisms aiming to explain their origin.

3. Data acquisition.

A total of 413 onshore (relative and absolute) gravity data were used in this study (Fig. 1). Then, we built the complete Bouguer anomaly map of El Hierro, which enabled us to generate a 3D density contrast model, obtained through a gravity data inversion procedure based on the genetic algorithm described by Montesinos et al., (2005a, 2006).

We used different data sources for this study. Gravity data were obtained from two main sources (Table 1). On the one hand, we used data from Spanish Geographic National Institute (IGN), 73 corresponding to the REDNAP, and 166 data acquired in different gravity campaigns carried out during years 2012 and 2013. On the other hand, we utilized 165 surface gravity values supplied by Montesinos et al., (2005a, 2006). As additional supporting information, 9 absolute gravity values, obtained during 2014, were included in the calculation process. Moreover, continuous gravity measurements and Earth's crustal response to tidal forces were analyzed in previous works using the LaCoste&Romberg Graviton-EG1194 and gPhone#054

relative gravimeters, both placed in the 'Aula de la Naturaleza' station during different periods of time (Arnoso et al., 2011; Sainz-Maza et al., 2014) (see Figure 1).

The 166 new relative gravity measurements were combined with simultaneous GPS observations made with a Trimble R4 GNSS 5800 receiver. Every GPS observation was linked to other GPS reference stations from IGN permanent network (see Figure 1) (López et al., 2012).

The new gravimetric measurements were conducted using always the same observational procedure, recording gravity values during 15-20 minutes intervals and GPS data at 1Hz logging frequency during the same time interval. The daily itineraries were designed to start and end at the same location every working day. Moreover, at least one of the intermediate points of each itinerary was re-observed for checking tares or changes in the gravimeter drift or jumps.

4. Data processing methodology.

GPS data processing was made through the Leica Geosystems software. As we already pointed out, every observation interval was compared to a minimum of 7 GPS reference stations placed in El Hierro. Thus, the coordinates of the observing points were determined with an error of 1 cm for the vertical component.

To homogenize the gravity data from all sources, old and new data were reprocessed using common procedures. Usual corrections were applied aiming to obtain the Complete Bouguer Anomaly (Torge, 1989). Earth tides and ocean tide loading effects were subtracted from the raw data according to standard models such as the Wenzel catalogue for Earth tides (Hartmann and Wenzel, 1995) and the FES04 global ocean tide loading model (Lyard et al., 2006). Gravimeter instrumental drift was modelled as linear trend (Torge, 1989). Moreover, all measurements were transferred to the terrain surface using the theoretical vertical gravity

gradient (-3.086 μGal/cm (1 μGal = 10^{-8} m/s^2)).

One of the most crucial stages of the processing to get precise complete Bouguer anomalies is the terrain correction. It is heavily influenced by the accuracy of the terrain model used (DEM). In the particular case of El Hierro, which is a small island with a very sharp topographic relief and surrounded by deep ocean, this correction plays an important role in the final anomaly value. In this regard, Figure 2 shows a synthetic example of the DEM influence in the nearby terrain correction applied over a point located near to a high terrain slope, as the case of El Golfo depression. Differences between the use of a 5m DEM model or a 25m DEM, change the order of the magnitude of the correction from 10^2 μGal to 10^3 μGal, assuming a synthetic model with rather conservative slopes (45º) compared with El Golfo escarpments (Figure 2).

We made the terrain correction modelling the topography based on the Kane grid (Kane, 1962). We divided the terrain in a great number of prismatic bodies, whose particular gravity attractions are easily manageable following the Nagy formula (Nagy, 1966):

$$\Delta g_p^k = G\rho|||x_i ln(y_i + r_i) + y_i ln(x_i + r_i) - z_i arcsin \frac{z_i^2 + y_i^2 + x_i y_i}{(y_i + r_i)\sqrt{z_i^2 + y_i^2}} |_{x_1}^{x_2} |_{y_1}^{y_2} |_{z_1}^{z_2} \quad (1)$$

where Δg_p^k is the gravity attraction of the *k*-prism over the *p*-gravity station, *G* is the Gravitational constant, ρ is the chosen terrain density and x_i, y_i and z_i, (i=1,2) are the limiting coordinates of the corresponding k-prism in each coordinate axis regard to the observed point. The r_i represents the radial distance between the k-prism center and the p-station.

To set up the heights of our terrain model, we used a 5x5m^2 DEM from IGN. We reproduced the first four square kilometers surrounding the observed point. Then, from 1km to 30 km of distance, a 50x50m^2 DEM was selected. Finally, a 500x500m^2 DEM was used from 30 km to 167 km. These distance values and DEMs were selected after several tests looking

for a better estimate of the terrain effect taking into account the former considerations and the computing time. The bathymetry corresponding to the offshore areas was modeled using data from GEBCO (General Bathymetric Chart of the Oceans; Weatherall et al., 2015).

Additional corrections were applied to the data, as the gravity influence of the atmospheric loading, calculated from the NOAA/NASA/USAF, 1976 atmosphere model. The Earth's curvature and bathymetry were also taking into account, both corrected according to Nowell, 1999. The final Bouguer anomaly map is shown in Figure 3 and in supplementary material 1.

One of the most controversial issues we needed resolve in this work was the suitability of mixing data from different sources and epochs, among which there were discernible gravity changes related to a seismo-volcanic process (Sainz-Maza et al. 2014). The existence of an observed common benchmark in all data sources simplified the problem. It was the Tanajara geodetic mark (see Figure 1). Gravity differences between campaigns at this point were used as the checking parameter to evaluate if the data is suitable to merge. Thus, the maximum observed gravity variation obtained from 2001 to 2013 was around -100 μGal. The main source of this change is probably the uplift of the island from 2011 to 2013: around 15 cm at this area (García-Cañada et al., 2014), which would be equivalent to about -50 μGal. Deformation between 2001 and 2011 as well as mass distribution changes (Sainz-Maza et al., 2014) and instrumental differences, could be responsible for the rest of the observed variation.

Considering that the magnitude of the main gravimetric anomalies is around 1 mGal, a difference of -100 μGals in gravity and 15 cm in height, can be considered acceptable in order to merge data from different epochs aiming to model the final complete Bouguer anomaly map with the resolution that is required in this study (Fig. 3).

Data inversion procedure was developed in two steps. Firstly, we used all the onshore gravity data obtained previously to the eruption of 2011 to obtain a preliminary structural

model. That is, data from REDNAP and data provided by Montesinos et al., 2005a, 2006. Secondly, we used this model as an input parameter in the inversion procedure of the new gravity data obtained after 2011. Since the aim of this model is to extend the information to the shallower sections of the model and to identify potential structures related to the rifts systems, data used were limited to onshore data, which are more homogeneously distributed and are more accurate. Marine gravity data helped to constrain the model in the offshore areas in Montesinos et al. (2005a; 2006).

The methodology used for the 3D gravity inversion was based on a genetic algorithm widely described in Montesinos et al. (2005b). Starting from an initial partition of the subsoil volume in prisms characterized by preliminary density contrast values, the algorithm performs successive modifications following an iterative process which uses three main operators: selection, mutation and crossover. In each step of the process, the algorithm seeks to minimize an error function (equation 2) which is determined by the difference between the gravity field generated using the prisms model configuration and the observed field gravity data.

$$\boldsymbol{F(m_k)} = (\mathbf{A}\boldsymbol{m_k} - \boldsymbol{g_{obs}} - \boldsymbol{G_m u})^{\boldsymbol{T}} \boldsymbol{E_{ss}^{-1}} (\boldsymbol{A m_k} - \boldsymbol{g_{obs}} - \boldsymbol{G_m u}) + \boldsymbol{\beta m_k^T C_M m_k} \quad (2)$$

Where g_{obs} is the calculated gravity anomaly values, $\boldsymbol{A} = \boldsymbol{A_{ij}}$ is an $i{\cdot}j$ matrix, which defines the gravity attraction divided by density unit at ith station due to the influence of the jth prism of the model, $\mathbf{G_m}$ represents the regional tendency defined by one constant term and u is an unitary vector. $\mathbf{E_{ss}}$ is a data error matrix obtained from a covariance analysis, β is an empirical parameter corresponding to the Tikhonov regularization technique (Schwarz, 1979). Finally, the uncertainty of the model is given by the m·m matrix C_M.

Initially, the process generates a population of distinct models (individuals), changing randomly the density of some cells. In every stage of the iterative process, individuals of the

corresponding population are evaluated and chosen using a selection operator (Michalewicz, 1994). It acts seeking the minimization of the error function $F(m_k)$ (see equation 2), selecting the individuals that best satisfy this minimization condition. Then, two genetic operators are introduced, mutation and crossover. They generate new individuals, which will be also evaluated. The mutation operator modifies randomly the density of some prisms of some models. It provides random diversity in the population and increases the sampled volume of the model space. Furthermore, crossover operator acts and exchanges information between several selected models. Then, the modified models are evaluated again with the unmodified ones, repeating the evolutionary process (selection/mutation/crossover).

The iterative process will continue until a predefined value of the error function is reached. Once this value is attained, a new stage of the process begins, looking for a model with a smoother geometry, defined by a smoothing operator which removes uncertainties of the model and avoids local minima (Montesinos et al. 2005a). Thus, this new operator is implemented which assigns each prism an averaged value of the density contrasts of the adjacent prisms. The process becomes iterative again with these smoothed individuals, which comprise a new population and it ends when the best individual from a population reaches to minimize the error function. At this point the process is finished and a 3D density contrast model of the subsoil is generated.

We applied this inversion algorithm using as input parameters: the new gravity data observed at El Hierro, a preliminary structural model obtained from data prior to 2011, and a maximum density contrast between ±350 kg m^{-3} regarding a mean density of 2510 kg m^{-3}. This density mean value was obtained from the minimum correlation between Bouguer anomaly and topography according to Nettleton (1939) methodology. Moreover, most of the points have a contiguous station nearest than 1000 m apart and the mean diameter of the survey is about 20000 m. It allowed to divide the local subsurface into 13874 rectangular prisms, with sides

ranging from 293m for some of the shallower elements (located at 1125 m a.s.l. in the highest zone of the island) to 1176 m for the deepest blocks (at -11000 m. b.s.l.). Once the inversion methodology was applied, the gravity data corresponding to the density contrast model fits to the observed data with a root mean square error under 500 μGal, indicating a good agreement between data and observations.

5. Results and discussion.

Intuitively, it seems reasonable that surface areas characterized by a concentration of volcanic vents along preferred directions, should display structural features connected to the observed alignments. Therefore, following the traces of the rifts from the surface to deeper regions, we should be able to image the internal structure and continuation with depth of these structures. Gravity inversion procedures offer the possibility to develop a structural model of the subsurface.

Most of the new gravity inversion results coincide with the findings from previously published works. The principal central structure, which is characterised by a high positive density contrast under the onshore part of the island (Montesinos et al., 2005a, 2006) is confirmed. Indeed, results from microseismic sounding reveal that this body forms a sort of funnel-shape structure under the central part of El Golfo and is rooted at large depths, at least up to a depth of 35 km, according to the model of Gorbatikov et al., 2013. Toward the surface, this body shows a more irregular geometry, becoming increasingly heterogeneous from intermediate depths (35-10 km) to shallowest levels (< 10km), where it exhibits a greater variability on the density contrast elements obtained from our model (Fig. 4). The high volume of onshore gravity data, and the more precise digital terrain and bathymetric models as well, have allowed us to obtain a model displaying a better image of the connection between the different shallower density layers towards the surface than in previous work of Montesinos et

al. (2006). This fact provided a visual argument to discuss about the relationship between the areas characterized by a high magmatic intrusive activity and the rifts.

From the comparison of Bouguer anomaly map with cones, fissures (Becerril et al., 2015) and seismicity (Dominguez et al., 2014) (Figure 3), it is easily distinguishable the lack of correlation between the distribution of cones observed at surface and that of gravimetric anomalies, but it should be taken into account that several huge landslides affected the island in the past, hiding and removing many cones. However, the distribution of fissures, over the onshore part of the island, offers a pattern in which most of these fissures are perpendicular to the contours lines of the gravity anomalies. It is not possible for us to discern any structural correlation between Bouguer anomalies and fissures, as these are also perpendicular to the topographical level lines. Finally, it seems that there is a clear connection between the seismicity occurred during 2011 and the highest Bouguer anomaly area, located at the center of the island, which could indicate that this anomaly is mainly generated by a structure that acted as a shield, impeding the vertical magma advance (see Martí et al., 2017).

From the horizontal layers displayed in Figure 4, it is remarkable that rift structures at surface, characterised by an upland topography covered by lots of aligned cones and fissures, do not exhibit significant correlations with any outstanding density contrast following the corresponding alignments. In order to see more clearly the distribution of the gravity anomaly sources at the shallower subsurface of El Hierro and to study the structure of the rift system in this island, we point out three vertical profiles where we have distinguished more remarkable features (Fig 5). Figure 5a shows a SW-NE profile marked by a high density contrast. Several apophysis connect this anomalous zone with the shallower parts of the model. Another interesting feature of this profile is the very shallow low density anomaly that corresponds to the Tanganasoga volcano surroundings, the largest recent volcanic edifice of El Hierro. This eruption took place along a N-S fissure with several eruptive vents, which originated the

accumulation of large volume of pyroclastic deposits (Carracedo et al., 2001). These low consolidated materials would be the origin of the observed low density structure.

The second selected profile (Fig. 5b) crosses northeastern rift zone. This profile shows a strong dominance of high density contrasts that reach the surface at various points in the surroundings of the Tiñor edifice area (Figure 1). This fact could suggest repeated magma injections filling this area following that alignment. From the Figure 5d showing the 3D density contrast model (see also supplementary material 2), it can be appreciated that this high density structure is an extension of one of the outgoing apophysis of the main high density structure which reaches the Northwest rift.

The third profile is shown in Fig. 5c. It corresponds to an alignment also characterized by high density contrasts which crosses the western rift zone. This alignment coincides with the one followed by the location of hypocenters during the seismicity previous to the volcanic eruption occurred during 2011-2012 (see Martí et al., 2013), with the difference that our gravity model describes shallower subsoil levels than the described by the seismicity. In this case, the high density structure only reaches an onshore area of the surface in a coastal area of the southern part of the island. It also shares with the other profiles the depth level where the structure begins to develop in a more heterogeneous way, which is placed around 2km b.s.l.

Finally, Figure 5d shows that the high density structure does not reach the surface at west and south rifts at the onshore part of the island. In turns, it seems to reach the northwest rift around a narrow area, where it extends toward the NW- SE as it can be seen in figure 5b.

The horizontal sections in the Figure 4 and the three vertical profiles shown in the Figure 5, provide a representative view of the 3D model of the distribution of the density contrasts inside El Hierro volcanic edifice (See a 3D visualization in supplementary material 2). This new accurate model reaches a depth of 7 km b.s.l. , so its represents the shallowest part of the system (in Montesinos et al., (2005a) it reaches to 10 km), which comprises from base to

top the uppermost layers of the pre-El Hierro basaltic crust, the pre-volcanic sedimentary layers, and the whole El Hierro volcanic edifice.

As mentioned before, the main density contrast corresponds to a funnel shaped positive anomaly that occupies most of the interior of the studied volume, showing a regular distribution from the bottom of the model to about 1-2 km b.s.l. We interpret this main anomaly as corresponding to the shallower magma accumulation zone that characterizes mature oceanic volcanoes such El Hierro (Klugel et al, 2015). This magma accumulation zone may had installed at pre-volcanic sedimentary layers (Klugel et al., 2015) and now forms the denser core of El Hierro shallow internal structure. From previous studies (Gorbatikov et al., 2013) it is known that this body continues to much greater depths, and probably connecting with deeper magma accumulation zones as envisaged by Klugel et al (2015) using petrological data. According to our model, this main anomalous body presents several apophysis at the upper part from 4000 m b.s.l onwards. They would be connected with different on-land and offshore zones at the surface of El Hierro edifice, and probably correspond to the main pathways that magma has used to reach the surface or a shallow reservoir, as also can be observed in the cones distribution in the surrounding bathymetry (Weatherall et al., 2015). The profile shown in Fig 5a, is consistent which the huge amount of dykes that are now exposed along the El Golfo landslide scar (Münn et al., 2006).

According to our model and focusing on results from density contrasts distribution, the rifts alignments, marked as blue dashed lines in Figure 1, are not highlighted by any density anomaly at intermediate depths, as it would be expected in case of being related to the direct ascend of deep magma to shallower depths. In addition, these alignments are not correlated with any relevant gravimetric anomaly (Figure 3). This lack of correlation is also present in other rift zones not related to volcanic islands as the Main Ethiopian Rift (Mazzarini et al., 2016). The connection between the shallower magma accumulation zones and the surface does

not occur along the whole rift structures but through well-defined channels that point to specific locations. The fact that the number of volcanic vents is quite large and covers most of the island surface along the rift zones suggests that the rift zones may have acted as channels to facilitate lateral magma migration at very shallow depths. Moreover, these zones would act as preferred sites of emplacement for dikes originating from very shallow secondary magma reservoirs. In summary, what we identify is a funnel-shape body that makes fingering at the surface to feed eruption. Magma is guided laterally from the finger tips to feed all the surface eruptions, being lateral guidance promoted by local stress field (ie rift zone) (Figure 6). A similar situation has been proposed for Tenerife using AMS data (Delcamp et al 2014).

This coincides with the interpretation of the rift zones in other ocean volcanic island such as Hawaii (Ryan, 1988) or La Reunion (Michon et al., 2015). In consequence, our results do not support the idea that El Hierro rift zones formed as consequence of mantle uplift but are more in favor of a much shallower origin (e.g.: Montesinos et al., 2005a; Münn et al., 2006; Gorbatikov et al., 2013; Becerril et al., 2015) probably related with the loading and unloading episodes and shallower processes that succeeded during the construction of El Hierro edifice. During the growing of volcano edifices, the local loading stress field favors the lateral displacement of the rising dykes causing eruptions away from the volcano's maximum loading area. Different experiments have reproduced this fact in the laboratory (Mathieu et al., 2008; Kervyn et al. 2009, Galland et al., 2009).

It is worth mentioning that SW-NE direction displayed in the Fig 5a, corresponds to the alignment along which the main positive density anomaly at depth connects with the onshore surface more frequently. It does not correspond to any rift, but it could be assimilated to a preferred direction of extensive fracturing already present in the island basement, as it occurs in other islands of the Canary Archipelago (Geyer and Martí, 2010; Geyer et al., 2016). This is the direction of the southern limit of the funnel shaped gravity anomaly and corresponds to part of

the El Hierro plumbing systems that would have acted as a main transport channel for deeper magmas and which would start to ramify towards other directions at much shallower depths. Comparatively, the shape of the northern limit of this density anomaly (see Supplementary Material 2) is clearly affected by the El Golfo landslide, which indicates that the structure of the plumbing systems was modified by this large mass wasting event. This supports the fact that the intermediate and shallower parts of the El Hierro plumbing system are controlled by the local stress field (i.e., loading and unloading processes), while the deepest part would be more controlled by the regional stress field (i.e, regional tectonic structures and mantle anomalies), as it seems to occur in other volcanic islands systems (Ryan, 1988; Michon et al., 2015)

6. Conclusions

To further investigate the internal structure of the El Hierro rifts system, previous 3D gravity inversion models of the island have been refined by adding new onshore gravity data, using a more precise terrain correction, and focusing the area of study on a more restricted region. This has permitted to elaborate a detailed 3D model of the shallower part of El Hierro volcanic edifice. The model obtained does not support the existence of three rift zones in El Hierro, as it could be deduced from the apparent orientation of eruption fissures vents location at surface. In our model these surface structures do not conform any density contrast or gravimetric anomaly that we could trace inside the volcanic system. On the contrary, the main anomaly we found agrees with previous gravity studies and it represents a central volume inside the edifice that probably corresponds to series of sills and other sheets intrusions forming as a whole a main magma accumulation zone between 2 to 7 km b.s.l. Magmas from this accumulation zone reach the surface through well located pathways apparently not corresponding to the surface rift zones, these last only contributing to distribute magma laterally when it arrives close to the surface. According to our results, the El Hierro rift zones

could not have a deep origin. They are more consistent to shallower processes (e.g.; sector collapses) that, in combination with the loading caused by the construction of the volcanic edifice and its subsequent basal spreading, may generate specific shallow extensional stresses able to open of the rift zones, thus controlling the location of most volcanic vents during the last constructive episode of the island.

Acknowledgements

This work was supported by IGN, CSIC and EC grant VUELCO, through the projects CGL2011-16144-E, CGL2015-63799-P, and REN2002-00544/RIES of the Spanish Ministry of Economy and Competitiveness. We want to thank the constructive comments made by Audrey Delcamp and Francesco Mazzarini which have considerably helped to improve the quality of this paper. We would also like to thank the Volcano Monitoring Group (IGN) for the support provided during the field surveys.

REFERENCES

Amelung, F., Yun, S. H., Walter, T. R., Segall, P., Kim, S. W., 2007, Stress Control of Deep Rift Intrusion at Mauna Loa Volcano, Hawaii, Science, Vol. 316, Issue 5827, pp. 1026-1030, DOI:10.1126/science.1140035.

Anguita, F., Hernán, F., 2000, The Canary Islands origin: a unifying model, J. Volcanol. Geotherm. Res., Vol. 103, Issues 1-4, pp. 1-26, DOI: 10.1016/S0377-0273(00)00195-5.

Arnoso, J., Benavent, M., Bos, M.S., Montesinos, F.G., Vieira, R., 2011. Verifying the body tide at the Canary Islands using tidal gravimetry observations, Journal of Geodynamics, Vol. 51(5), 358–365, doi:10.1016/j.jog.2010.10.004.

Becerril, L., Galindo, I., Martí, J., Gudmundsson, A., 2015, Three-armed rifts or masked radial pattern of eruptive fissures? The intriguing case of El Hierro volcano (Canary Islands), Tectonophysics, Vol. 647–648, pp. 33–47, DOI:10.1016/j.tecto.2015.02.006.

Becerril, L., Galve, J. P., Morales, J.M., Romero, C., Sánchez, N., Martí, J., Galindo, I., 2016, Volcano-structure of El Hierro (Canary Islands), Journal of Maps, pp.1-10, DOI:10.1080/17445647.2016.1157767.

Blanco-Montenegro, I., Nicolosi, I., Pignatelli, A., Chiappini, M., 2008, Magnetic imaging of the feeding system of oceanic volcanic islands: El Hierro (Canary Islands), Geophys. J. Int., Vol. 173, Issue 1, pp. 339–350, DOI:10.1111/j.1365-246X.2008.03723.x.

Bonali, F.L., Corazzato, C., Tibaldi, A., 2011, Identifying rift zones on volcanoes: an example from La Réunion Island, Indian Ocean, Bull. Volcanol., Vol. 73, Issue 3, pp. 347–366, DOI: 10.1007/s00445-010-0416-1.

Carracedo, J.C., 1994, The Canary Islands: an example of structural control on the growth of large oceanic-island volcanoes, J. Volcanol. Geotherm. Res., Vol. 60, pp. 225-241, DOI: 10.1016/0377-0273(94)90053-1.

Carracedo, J.C., 1996, Morphological and structural evolution of the western Canary Islands: Hotspot induced three armed rifts or regional tectonic trends?, J. Volcanol. Geotherm. Res., Vol. 72, Issue 1, pp. 151-162, DOI: 10.1016/0377-0273(95)00080-1.

Carracedo, J. C., Rodriguez-Badiola, E., Guillou, H., de La Nuez, J. and Pérez Torrado, F.J., 2001, Geology and volcanology of La Palma and El Hierro, Western Canaries, Estud. Geol., Vol. 57, Issues 5-6, pp. 175-273.

Carracedo, J.C., Guillou, H.,Nomade, S., Rodríguez-Badiola, E.,Pérez-Torrado, F.J.,Rodríguez-González, A.,Paris, R.,Troll, V.R.,Wiesmaier, S.,Delcamp, A.,Fernández-Turiel, J.L., 2011, Evolution of ocean-island rifts: The northeast rift zone of Tenerife, Canary Islands, Vol.123, Issue 3-4, pp. 562-584, DOI:10.1130/B30119.1

Carter, A., van Wyk de Vries, B., Kelfoun, K.,Bachèlery P., Briole P., 2007, Pits, rifts and slumps: the summit structure of Piton de la Fournaise, Bull. Volcanol., Vol. 69, Issue 7, pp. 741-756, DOI: 10.1007/s00445-006-0103-4 .

Corazzato, C., A. Tibaldi, 2006, Fracture control on type, morphology and distribution of parasitic volcanic cones: an example from Mt. Etna, Italy, J. Volcanol. Geotherm. Res., Vol. 158, Issues 1–2, pp. 177–194, DOI:10.1016/j.jvolgeores.2006.04.018.

Delcamp, A., Troll , V. R., van Wyk de Vries, B., Carracedo, J. C., Petronis, M. S., Pérez-Torrado, F. J., 2010, Vertical axis rotation of the upper portions of the north-east rift of Tenerife Island inferred from paleomagnetic data, Tectonophysics, Vol. 492, Issues 1–4, pp. 40–59, DOI:10.1016/j.tecto.2010.04.020.

Delcamp, A., Petronis, M. S., Troll , V. R., Carracedo, J. C., van Wyk de Vries, B., Pérez-Torrado, F. J., Deegan, F. M., 2012, Dykes and structures of the NE rift of Tenerife, Canary Islands: a record of stabilisation and destabilisation of ocean island rift zones, Bull. Volcanol., Vol. 74, Issue 5, pp. 963–980, DOI:10.1007/s00445-012-0577-1.

Delcamp A., Petronis M.S., Troll V.R., 2014. Magmatic flow in shallow level basaltic dykes using AMS and field analyses: North-East Rift Zone, Tenerife, Canary Islands, Spain. Geol.Soc. London 396: Special issue "The Use of Palaeomagnetism and Rock Magnetism to Understand Volcanic Processes". DOI 10.1144/SP396.2

Domínguez Cerdeña, I., del Fresno, C. and Gomis Moreno, C. 2014. Seismicity patterns prior to the 2011 El Hierro Eruption, B. Seismol. Soc. Am., 104 (1), 567-575; DOI: 10.1785/0120130200.

Fiske, R. S., Jackson, E.D., 1972, Orientation and growth of Hawaiian volcanic rifts: the effect of regional structure and gravitational stresses, Proc. R. Soc. London, Ser. A, Vol. 329, pp. 299-326, DOI:10.1098/rspa.1972.0115.

Folger, D.W., McCullough, J.R., Irwin, B.J., Dodd, J.E., Strahle, W.J., Polloni, C.F., Bouse, R.M., 1990. Map showing free-air gravity anomalies around the Canary Islands, Spain, Miscellaneous Field Studies Map, MF-2098-B, p. (1 sheet), U.S. Geol. Surv., United States.

Galland, O., Planke, S., Neumann, E.-R., Malthe-Sørenssen, A., 2009. Experimental modelling of shallow magma emplacement: application to saucer-shaped intrusions. Earth Planet. Sci. Lett. 277, 373–383. DOI: 10.1016/j.epsl.2008.11.003

García-Cañada, L., García-Arias, M.J., Pereda de Pablo, J., Lamolda, H., López, C., 2014, Different deformation patterns using GPS in the volcanic process of El Hierro (Canary Island) 2011-2013, Geophysical Research Abstracts, Vol. 16, EGU2014-15791

García-Yegüas, A., Ibáñez, J.M., Koulakov, I., Jakovlev, A., Romero-Ruiz, M.C., Prudencio, J., 2014, Seismic tomography model reveals Mantle magma source of recent volcanic activity at El Hierro Island (Canary Islands, Spain), Geophys. J. Int., Vol. 199, Issue 3, pp. 1739-1750, DOI:10.1093/gji/ggu339.

Gee, M. J. R., Masson, D. G., Watts, A. B., Mitchell, N. C., 2001, Offshore continuation of volcanic rift zones, El Hierro, Canary Islands, J. Volcanol. Geotherm. Res., Vol. 105, Issues 1–2, pp. 107–119, DOI: 10.1016/S0377-0273(00)00241-9.

Geyer, A., Martí, J., 2010, The distribution of basaltic volcanism on Tenerife, Canary Islands: Implications on the origin and dynamics of the rift systems, Tectonophysics, Vol. 483, Issues 3–4, pp 310–326, DOI:10.1016/j.tecto.2009.11.002.

Geyer, A., Martí, J. and Villaseñor, A., 2016, First-order estimate of the Canary Islands plate-scale stress field: Implications for volcanic hazard assessment, Tectonophysics, Vol. 679, pp. 125–139, DOI:10.1016/j.tecto.2016.04.010.

Gorbatikov, A.V., Montesinos, F.G., Arnoso, J., Stepanova, M.Yu., Benavent, M., Tsukanov, A.A., 2013, New features in the subsurface structure model of El Hierro island (Canaries) from low-frequency

microseismic sounding. An insight into the 2011 seismo-volcanic crisis, J. Surv. Geophys., Vol. 34, Issue. 4, pp. 463–489, DOI: 10.1007/s10712-013-9240-4.

Guillou, H., Carracedo, J.C., Pérez-Torrado, F., Rodríguez Badiola, E., 1996, K-Ar ages and magnetic stratigraphy of a hotspot-induced, fast-grown oceanic island: El Hierro, Canary Islands, J. Volcanol. Geotherm. Res., Vol. 73, Issues 1–2, pp. 141-155, DOI: 10.1016/0377-0273(96)00021-2.

Hartmann, T., Wenzel, H., 1995, The HW95 tidal potential catalogue, Geophys. Res. Lett., Vol. 22, Issue 24, pp. 3553-3556, DOI: 10.1029/95GL03324.

Hernández-Pacheco, A., 1982, Sobre una posible erupción en 1793 en la isla de El Hierro (Canarias), Estudios Geológicos, Vol. 38, Issues 1-2, pp. 15-26.

Kane, M.F., 1962, A Comprehensive System of Terrain Corrections Using a Digital Computer, Geophysics., Vol. 27, Issue 4, pp. 455–462., DOI:10.1190/1.1439044.

Kervyn, M., Ernst, G.G.J., van Wyk de Vries, B., Mathieu, L., Jacobs, P., 2009. Volcano load control on dyke propagation and vent distribution: insights from analogue modeling. J. Geophys. Res. 114, B03401. DOI: 10.1029/2008jb005653.

Klugel, A., Longpré, M. A., García-Cañada, L., Stix, J., 2015, Deep intrusions, lateral magma transport and related uplift at ocean island volcanoes, Earth and Planetary Science Letters, Vol.431, pp. 140–149, DOI:10.1016/j.epsl.2015.09.031.

Lipman, P.W., Calvert, A.T., 2011, Early growth of Kohala volcano and formation of long Hawaiian rift zones, Geology, Vol. 39, Issue 7, pp. 659-662, DOI:10.1130/G31929.1 .

Lonsdale, P., 1988, Structural patterns of the Galapagos Microplate and evolution of the Galapagos triple junction, J. Geophys. Res. Solid Earth, Vol. 93, Issue B11, pp. 13551–13574, DOI: 10.1029/JB093iB11p13551.

López, C., Blanco, M.J., Abella, R., Brenes, B., Cabrera Rodríguez, V.M., Casas, B., Domínguez Cerdeña, I., Felpeto, A., Fernández de Villalta, M., del Fresno, C.; et al. , 39., 2012, Monitoring the

volcanic unrest of El Hierro (Canary Islands) before the onset of the 2011-2012 submarine eruption, Geophys. Res. Lett., Vol. 39, Issue 13, DOI:10.1029/2012GL051846.

Lyard,F., Lefevre, F., Letellier T., Francis O., 2006, Modelling the global ocean tides: modern insights from FES2004, Ocean Dynamics, Vol. 56, pp. 394-415, DOI:10.1007/s10236-006-0086-x.

MacDonald, G.A., 1972, Volcanoes, Prentice-Hall Inc Englewood Cliffs (510PP.).

Martí, J., Pinel, V., López, C., Geyer, A., Abella, R., Tárraga, M., Blanco, M.J., Castro, A., Rodríguez, C., 2013, Causes and mechanisms of the 2011–2012 El Hierro (Canary Islands) submarine eruption, J. Geophys. Res. Solid Earth, Vol. 118, Issue 3, pp. 823–839, DOI:10.1002/jgrb.50087.

Martí, J., Villaseñor, A., Geyer, A., López, C., and Tryggvason, A., 2017, Stress barriers controlling lateral migration of magma revealed by seismic tomography, Scientific Reports, 7, 40757, DOI: 10.1038/srep40757

Masson, D.G., 1996, Catastrophic collapse of the flank of El Hierro about 15,000 years ago, and the history of large flank collapses in the Canary Islands, Geology, Vol. 24, Issue 3, pp. 231-234, DOI:10.1130/0091-7613(1996)?024<0207:CNEAAA>2.3.CO;2.

Mathieu, L., van Wyk de Vries, B., Holohan, E.P., Troll, V.R., 2008. Dykes, cups, saucers and sills: analogue experiments on magma intrusion into brittle rocks. Earth Planet. Sci. Lett. 271, 1–13. DOI: 10.1016/j.epsl.2008.02.020.

Mazzarini, F., LeCorvec, N., Isola, I. Favalli, M., 2016, Volcanic field elongation, vent distribution, and tectonic evolution of a continental rift: The Main Ethiopian Rift example, Geosphere, Vol. 12, Issue 3, pp. 706-720, DOI: 10.1130/GES01193.1.

Michalewicz, Z., 1994, Genetic algorithms + Data structures = Evolution programs, Springer- Verlag, Berlin, second extended edition, 340 pp.

Michon, L., Ferrazzini, V., Di Muro, A., Villeneuve, N., Famin, V., 2015, Rift zones and magma plumbing system of Piton de la Fournaise volcano: How do they differ from Hawaii and Etna?, J. Volcanol. Geotherm. Res., Vol. 303, pp. 112–129, DOI:10.1016/j.jvolgeores.2015.07.031.

Montesinos, F.G., Arnoso J., Benavent M., 2005a, New study of the local gravity field of El Hierro (Canary Islands), Física de la Tierra, Vol.17, pp.113-117.

Montesinos, F.G., Arnoso, J., Vieira, R., 2005b, Using a genetic algorithm for 3-D inversion of gravity data in Fuerteventura, J. Earth Sci., Vol. 94, Issue 2, pp. 301-316, DOI:10.1007/s00531-005-0471-6.

Montesinos, F.G., Arnoso J., Benavent M., Vieira R., 2006, The crustal structure of El Hierro (Canary Islands) from 3-D gravity inversion, J. Volcanol. Geotherm. Res., Vol. 150, Issues 1–3, pp. 283–299, DOI:10.1016/j.jvolgeores.2005.07.018.

Münn, S., Walter, T.R., Klügel, A., 2006, Gravitational spreading controls rift zones and flank instability on El Hierro, Canary Islands, Geological Magazine, Vol. 143, pp. 257-268, DOI:10.1017/S0016756806002019.

Nagy, D., 1966, The prism method for terrain corrections using digital computers, Pure Appl. Geophys., Vol. 63, Issue 1, pp. 31–39, DOI:10.1007/BF00875156.

Nettleton, L.L., 1939, Determination of density for reduction of gravitimeter observations, Geophysics., Vol. 4, issue 3, p. 176. , DOI:10.1190/1.1437088 .

NOAA/NASA/USAF. U.S. Standard Atmosphere 1976. Washington, DC; 1976.

Nowell D.A.G., 1999, Gravity terrain corrections-an overview, Journal of Applied Geophysics, Vol. 42, Issue 2, pp. 117–134, DOI:10.1016/S0926-9851(99)00028-2.

Pellicer, M.J., 1977, Estudio volcanológico de la isla de El Hierro (Islas Canarias), Estudios Geológicos, Vol. 33, Issue 2, pp. 181.

Rittmann, A. , 1973, Structure and evolution of Mount Etna, Phil. Trans. Roy. Soc., London, Vol. 274, pp. 5-16.

Ryan, M.P., 1988, The mechanics and three-dimensional internal structure of active magmatic systems: Kilauea volcano, Hawaii, J. Geophys. Res. Solid Earth, Vol. 93, Issue B5, pp. 4213–4248, DOI: 10.1029/JB093iB05p04213.

Sainz-Maza, S., Arnoso, J., Gonzalez, F. G., Martí, J., 2014, Volcanic signatures in time gravity variations during the volcanic unrest on El Hierro (Canary Islands), J. Geophys. Res. Solid Earth, Vol. 119, Issue 6, pp. 5033–505, DOI:10.1002/2013JB010795.

Schwarz, K.P., 1979, Geodetic improperly posed problems and their regularization, Boll. Geodyn. Sci. Aff, Vol. 38, pp. 389-416.

Soriano, C., Beamud, E., Garcés, M., 2008, Magma flow in dikes from rift zones of the basaltic shield of Tenerife, Canary Islands: implications for the emplacement of buoyant magma, J. Volcanol. Geotherm. Res., Vol. 173, Issues 1–2, pp. 55–68, DOI:10.1016/j.jvolgeores.2008.01.007.

Tibaldi, A., Corazzato, C., Apuani, T., Cancelli, A., 2003, Deformation at Stromboli volcano (Italy) revealed by rock mechanics and structural geology, Tectonophysics, Vol. 361, Issues 3–4, pp.187–204, DOI:10.1016/S0040-1951(02)00589-9.

Tibaldi, A., Bonali, F.L., Corazzato, C., 2014, The diverging volcanic rift system, Tectonophysics, Vol. 173, Issues 1–2, pp. 55–68, DOI:10.1016/j.tecto.2013.11.023.

Torge, W., 1989, Gravimetry, Walter de Gruyter & Co. Publisher, Berlin, Germany..

Urgeles R., Canals M., Baraza J., Alonso B., Masson D.G., 1997, The most recent megalandslides of the Canary Islands: El Golfo debris avalanche and Canary debris flow, west El Hierro Island, J. Geophys. Res. Solid Earth, Vol. 102, Issue B9, pp. 20305–20323, DOI: 10.1029/97JB00649.

Villasante-Marcos, V., Pavón-Carrasco, F.J., 2014, Paleomagnetism constraints on the age of Lomo Negro volcanic eruption (El Hierro, Canary Islands), Geophys. J. Int., Vol. 193, Issue 3, pp.1497-1514, DOI:10.1093/gji/ggu346.

Walker, G.P.L., 1999, Volcanic rift zones and their intrusion swarms, J. Geophys. Res. Solid Earth, Vol. 94, Issues 1–4, December 1999, Pages 21–34, DOI: 10.1016/S0377-0273(99)00096-7.

Walter, T. R., 2003, Buttressing and fractional spreading of Tenerife, an experimental approach on the formation of rift zones, J. Geophys. Res. Solid Earth, Vol. 30, Issue 6, DOI: 10.1029/2002GL016610.

Walter, T.R., Troll, V.R., 2003, Experiments on rift zone evolution in unstable volcanic edifices, J. Geophys. Res. Solid Earth, Vol. 127, Issues 1-2, pp.107-120, DOI: 10.1016/S0377-0273(03)00181-1.

Walter, T.R., Troll, V.R., Cailleau, B., Belousov, A., Schmincke, H.U., Amelung, F., Bogaard, P., 2005, Rift zone reorganization through flank instability in ocean island volcanoes: an example from Tenerife, Canary Islands, Bull. Volcanol., Vol. 67, Issue 4, pp. 281-291, DOI: 10.1007/s00445-004-0352-z.

Weatherall, P., Marks, K. M., Jakobsson, M., Schmitt, T., Tani, S., Arndt, J. E., Rovere, M., Chayes,D., Ferrini V., Wigley, R., 2015, A new digital bathymetric model of the world's oceans, Earth and Space Science, Vol. 2, Issue 8, pp. 331-345, DOI:10.1002/2015EA000107.

Table 1: Data sources used in previous and current works. In 2014, we measured absolute gravity values for first time in El Hierro Island, which supported the quality of the relative gravity data.

Data Source	Gravimeter	Number of data
Previous works		
Montesinos et al., (2005a, 2006)	LaCoste&Romberg, models G933 and Graviton-EG1194	165
	Marine gravity data (U.S. Geological Survey; Folger et al., 1990)	257
New used data (All from IGN networks)		
REDNAP	Lacoste&Romberg gravimeters	73
Relative (2012-2013)	Scintrex CG5#811 (http://www.scintrexltd.com/gravity.html)	166
Absolute (2014)	A10#006 (http://www.microglacoste.com/a10.php)	9 (http://www.ign.es)

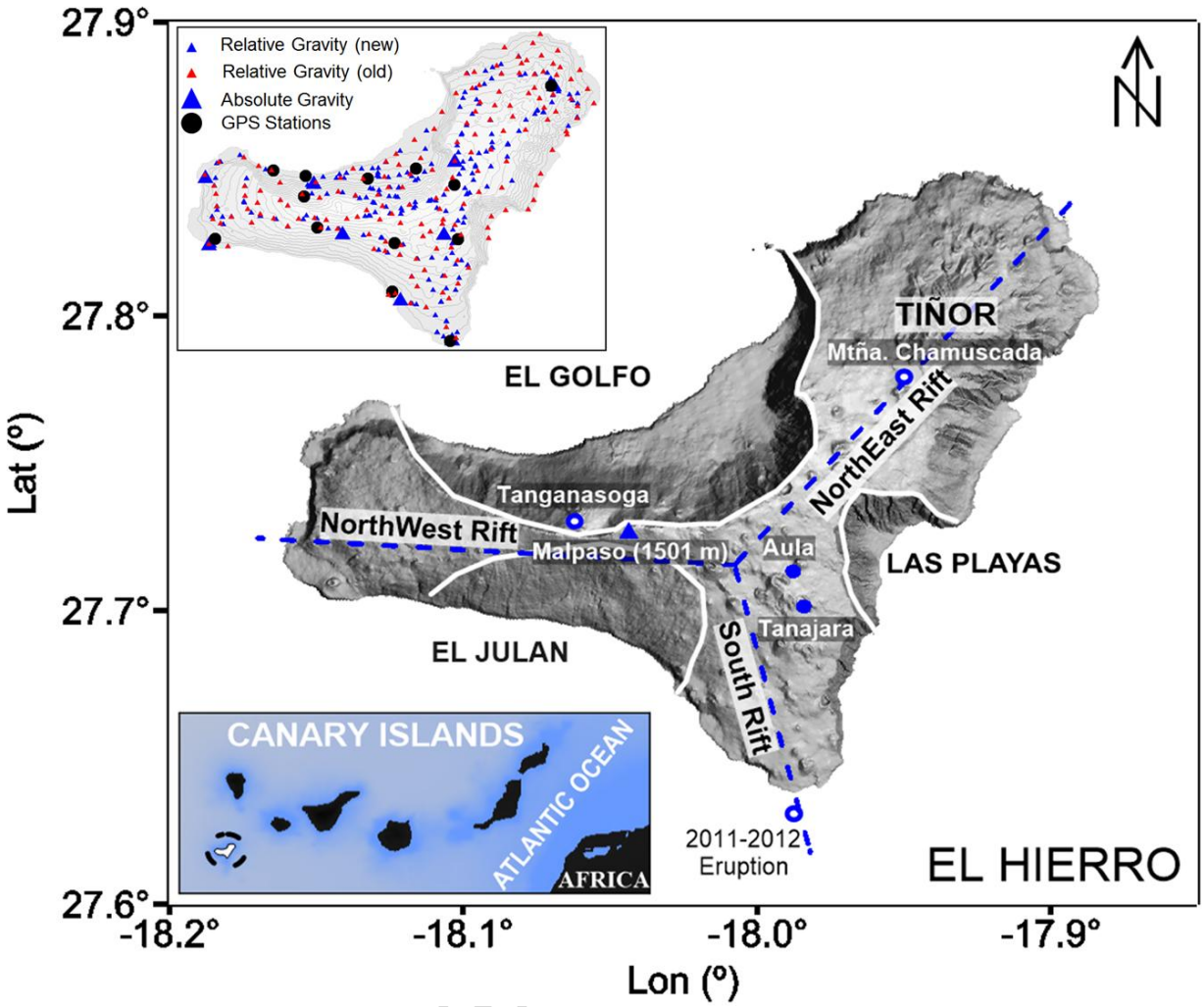

Figure 1. Shaded relief of El Hierro Island indicating its main morphological features (embayments of El Golfo, El Julan, and Las Playas, the volcanic rift systems are shown as blue dashed lines). Locations of Quaternary eruptions, Mtña. Chamuscada, Tanganasoga and 2011-2012 submarine eruption, are highlighted as blue-white circles. The highest location of the island, Malpaso, appears as a blue triangle. Tiñor volcanic area is indicated at the northeast of the map. The gravimetric observations used in this work, the location of absolute and relative gravity measurements and as the GPS reference stations are displayed at the top left corner. Aula and Tanajara points are main gravity benchmarks, so they are indicate outside of the inset figure to get a better visualization.

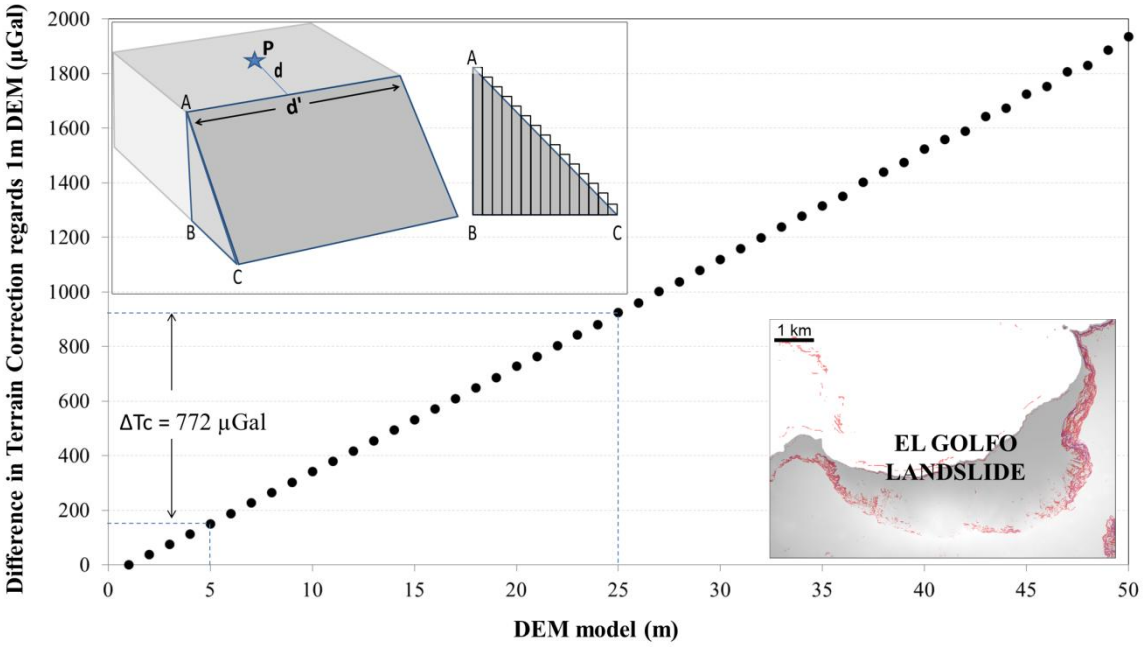

Figure 2. Synthetic example the influence of the Digital Elevation Models (DEM) over the Terrain Correction value. The upper-left corner of the plot shows a model where P represents the gravity benchmark, d is the distance to an abrupt depression rim (here we use 100 m) and d' is the length of the rim (we use a value 4 km, simulating only a little portion of El Golfo rim). A slope of 45o was selected for the example, which is modeled using prismatic bodies. In the lowest-right corner a detailed picture of El Golfo area from El Hierro Island is represented, and the slopes which are equal or greater than 45º are painting in red color. Maximum slope values identified are nearest to 84º. The graphic displays the change occurred on Terrain Correction calculated as function of the DEM model used. In this case, the variation in the final value of the Terrain Correction when using a 5 m DEM or a 25 m DEM is about 772 µGal.

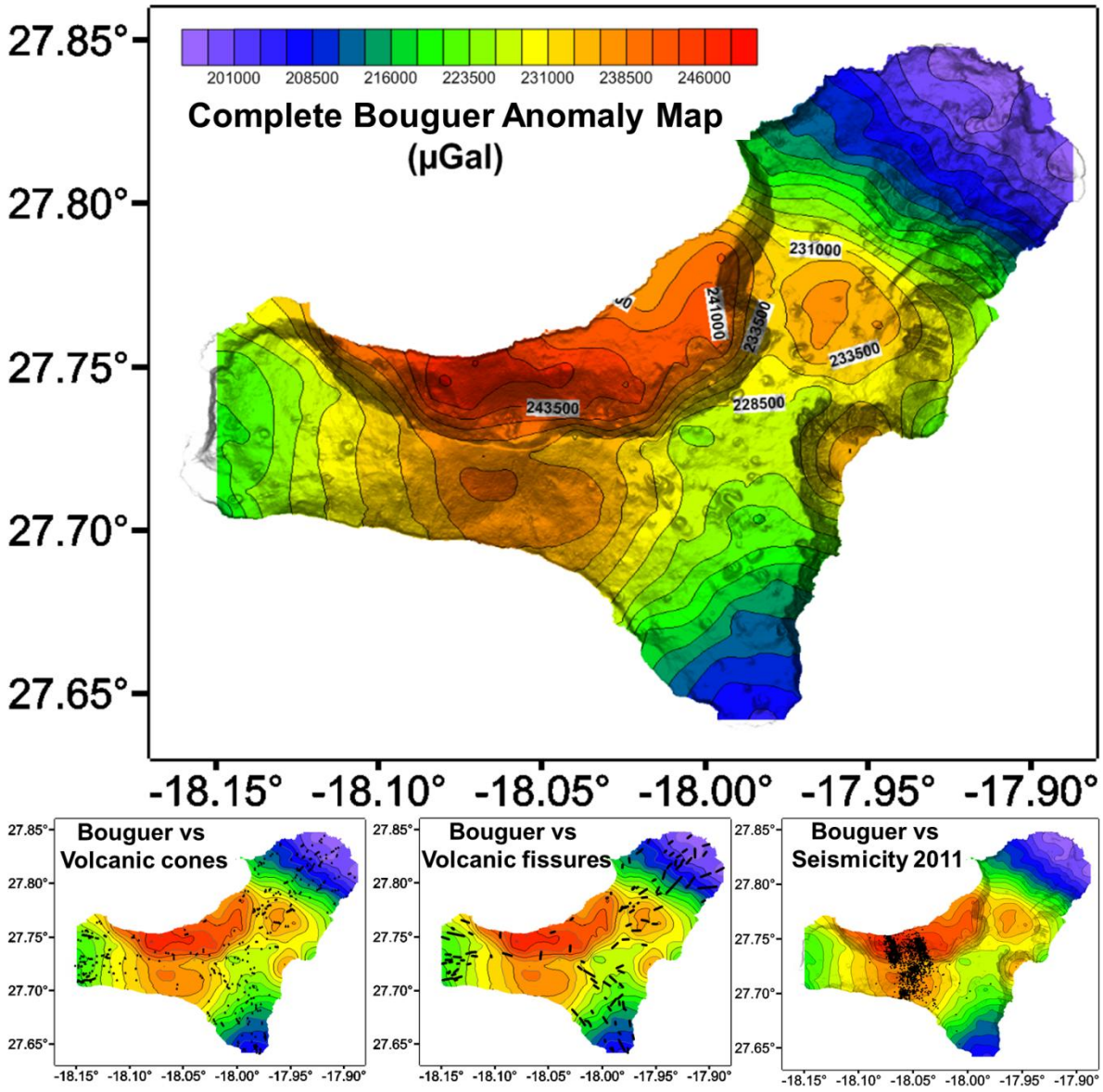

Figure 3. Complete Bouguer anomaly map for the onshore part of El Hierro Island. It shows maximum differences of about 50 mGal in the gravity anomaly. It is clearly visible as the highest anomaly values are related to the giant landslides of El Golfo, El Julan, and Las Playas. Below the Bouguer anomaly map, it is showed the comparison of the anomalies with the distribution of cones and fissures identified at surface (Becerril et al., 2015), and with the seismicity epicentres previous to the 2011 eruption bellow the onshore part of the island (Domínguez Cerdeña et al., 2014).

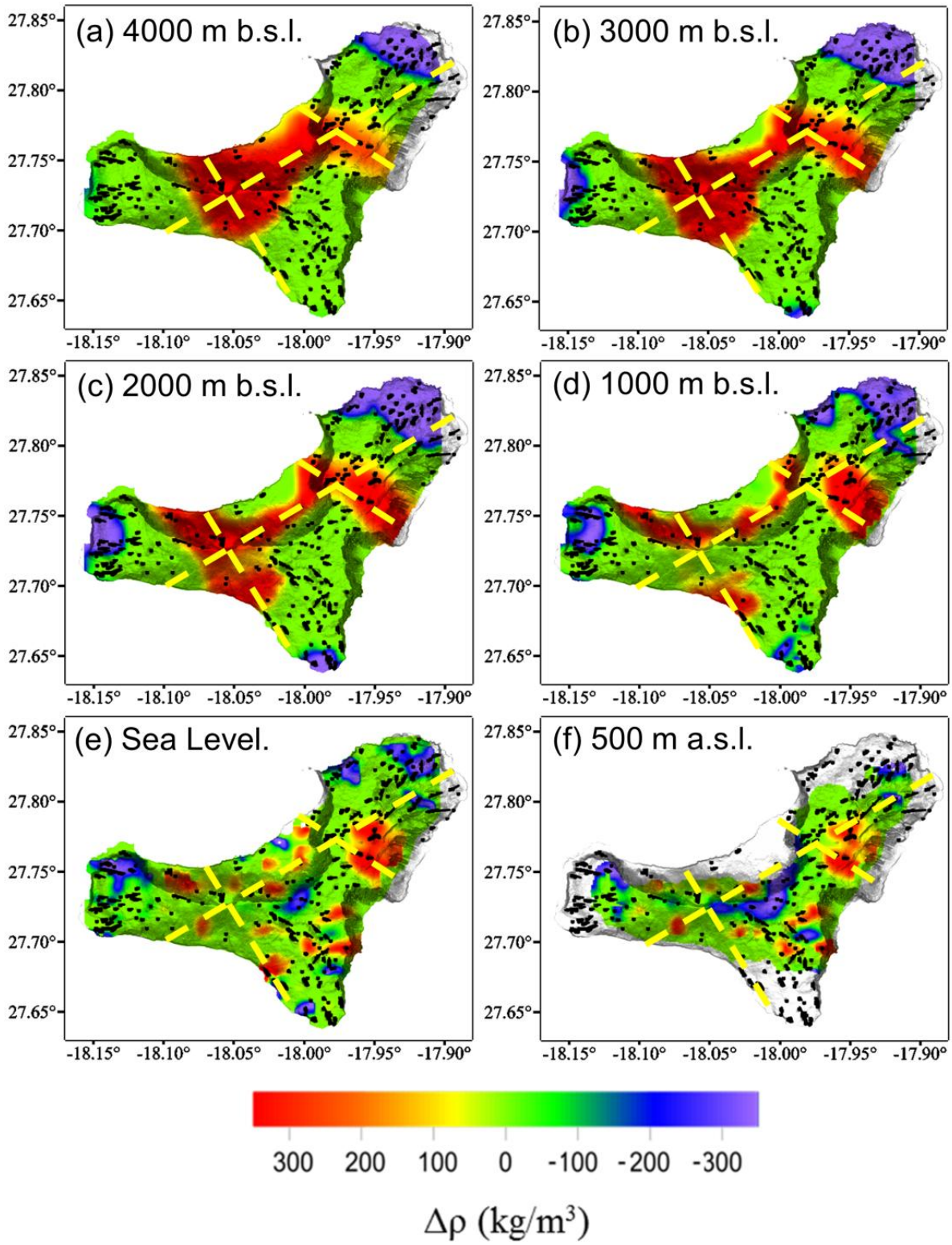

Figure 4. Horizontal sections of the density model every 1000 m obtained through the genetic inversion procedure from 4000 m b.s.l. An additional section at 500 m a.s.l has been included in order to display the shallower part of the model. Yellow dashed lines point out zones or alignments of structures where high densities are outstanding. The dense core body obtained at

depth from previous models (Montesinos et al., 2006) shows such of branched development as it raises. This effect becomes evident from 4000 m b.s.l, increasing the heterogeneity at 2000 m b.s.l. to the surface. The spatial distribution of cones and fissures are overlapping to the figures.

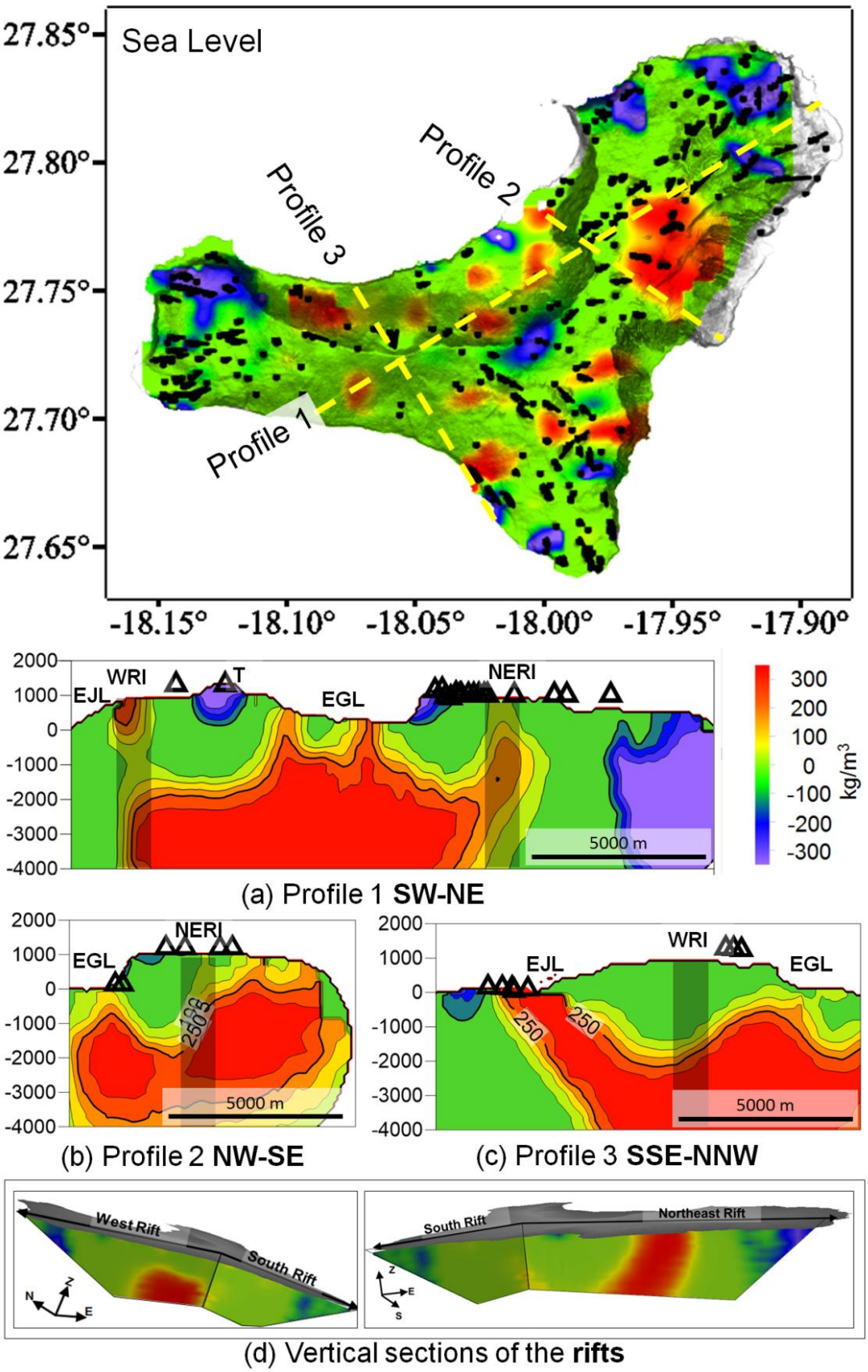
Sea Level
Profile 1
Profile 2
Profile 3
27.85°
27.80°
27.75°
27.70°
27.65°
-18.15°
-18.10°
-18.05°
-18.00°
-17.95°
-17.90°
WRI
T
EJL
EGL
NERI
5000 m
300
200
100
0
-100
-200
-300
kg/m3
(a) Profile 1 SW-NE
(b) Profile 2 NW-SE
(c) Profile 3 SSE-NNW
West Rift
South Rift
Northeast Rift
(d) Vertical sections of the rifts

Figure 5. Different profiles inferred using the density model. WRI and NERI are the corresponding intersections of the profile with the western and northeastern rift, which are indicated by shadow grey color. EGL and EJL correspond to El Golfo and El Julan landslides areas and T represents the Tanganasoga volcano. Black points in the first map and black triangles in the profiles indicate where volcanic cones are present at surface. (a) SW-NE profile, showing the dense core part of the subsurface and its branched form toward the surface. According to the number of apophysis of this profile, it seems to be the preferred orientation for magmatic intrusions from deeper areas. (b) NW-SE profile cutting the eastern rift of the island. A dense structure is now located with its lower part in a higher position. (c) This is SSE-NNW profile crossing El Hierro western rift area. Dense core structure seems is extended toward north and south parts of the island. (d) Vertical sections under the rift areas. High density structure seems to reach the surface only at Northwest rift, where the maximum extension for this structure follows along the profile displayed in (5b).

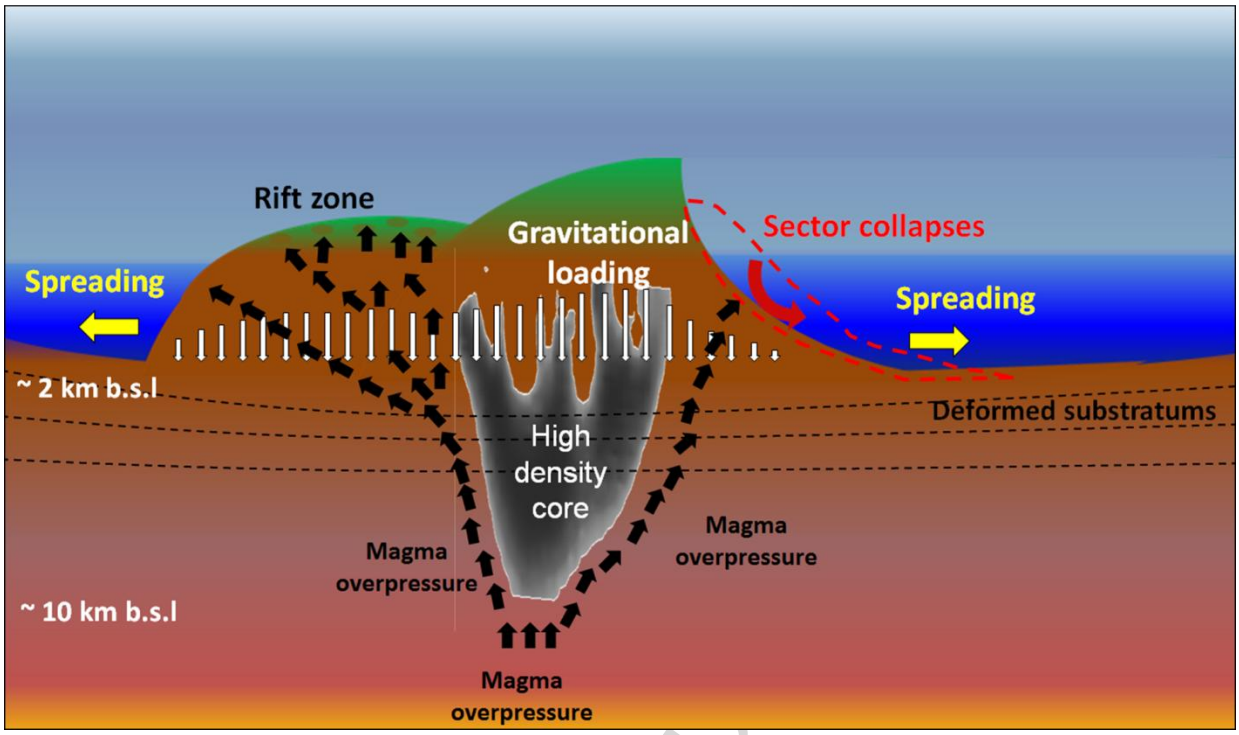

Figure 6. The model suggested establishes the final path followed by magma as determined by the final combination of various forces and the interposed structures in its way. High density structures obstruct the vertical buoyancy of the lower density magma. When magma reaches shallower lever its overpressure is favored by the gravitational loading, and the distribution (geometry) of the collapsed sector contributes to generate extensional stresses able to open the rift zones thus allowing magma to be distributed laterally.